

Geometric Characteristics of the Early Products of ALOS PRISM

Izumi KAMIYA

Abstract

An orientation program developed for ALOS PRISM was applied to a triplet of the early product of ALOS PRISM to clarify the geometric characteristics of the sensor. Errors of single image observation were 1.0 km before adjustment. The geometric errors were likely caused by rotation of radiometers and by mis-alignment of CCDs on the focal plane. Adjusting the rotation of the radiometers, residuals of single image observation were 4.9 m in the horizontal, and residuals of triplet image observation were 2.9 m in the horizontal and 3.2 m in the vertical, respectively. East–west distributed control points are necessary to adjust the radiometer rotation, especially two pairs of east and west control points are recommended.

1. Introduction

JAXA (Japan Aerospace Exploration Agency) launched the ALOS (Advanced Land Observing Satellite) on January 24, 2006. The satellite has three earth observation sensors: PRISM, AVNIR-2 and PALSAR.

PRISM (Panchromatic Remote Sensing Instruments for Stereo Mapping) consists of forward-looking, nadir-looking and backward-looking radiometers. PRISM observes the ground from 3 directions within an orbit using the 3 radiometers. Each radiometer has 6 or 8 CCDs on its focal plane (Earth Observation Research Center, JAXA, 2006). Usually, 4 CCDs are used for a radiometer. Pixel size is designed to be 2.5 m. One of the most important objectives of PRISM is medium-scale mapping and DEM production without ground control points.

The position of the satellite is obtained by GPS receivers, and the attitude by star trackers and gyros. In addition, ADS (Angular Displacement Sensor) is directly mounted on PRISM to measure high-frequency oscillation.

An orientation program with open algorithms for ALOS PRISM was developed in order to determine error factors and to improve geometric accuracy. The program was verified before the launch using simulation data which were obtained from LHSystems' ADS40 airborne digital sensor (Eckardt et al., 2000). ADS40 is a three-line stereo sensor like PRISM. The program

worked well for the simulation data, and clarified error factors of the simulation data (Kamiya, 2005, 2006).

The orientation program was applied to early products of PRISM, which was obtained and produced in the calibration/validation phase. This paper reports the result of the application.

A DEM/orthoimage generation program was also developed and checked successfully using simulation data from ADS40 (Kamiya, 2006). The orientation program and DEM/orthoimage generation program are expected to enable mapping from PRISM images without requiring a digital stereo plotter.

2. Algorithm

The adjustment of the orientation is a kind of bundle adjustment for a push-broom sensor. Though the position and attitude of the satellite are provided in the standard product of PRISM and these data are expected to be accurate, the adjustment may assume errors of the position and attitude as polynomials of time.

The adjustment always assumes errors of image observation, and may additionally assume the following errors: position and attitude of the satellite, ground coordinates of the control points, mounting angles of the radiometers, the principal distances, and the principal positions.

Corrections of aberration, atmospheric effect, and earth rotation are necessary for absolute orientation of PRISM images. These effects are, however, almost the

same in a radiometer, which means no effect after the adjustment using ground control points. The largest one, effect of aberration, was evaluated to be a maximum of 20 m. Therefore, these corrections are not actually implemented now.

3. Used data

3.1 PRISM data

A triplet set of PRISM data observed at Fukuoka, Japan (Fig. 1) was used. The data are standard products in level 1B1, which is radiometrically corrected and geometrically uncorrected. The data are some of the early PRISM products which have "ALOS precision attitude determination value." ADS data were, however, not used to determine the attitude.

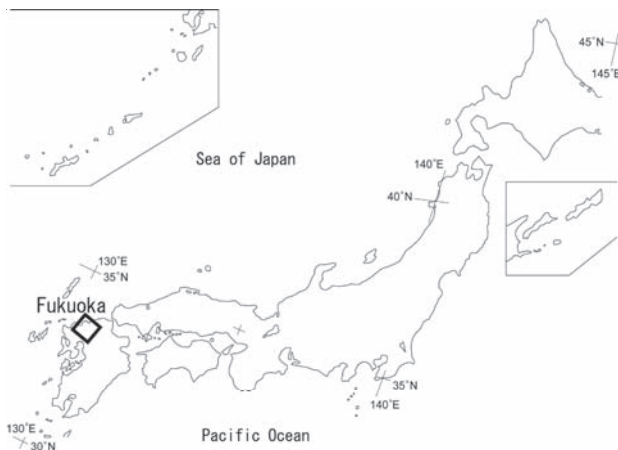
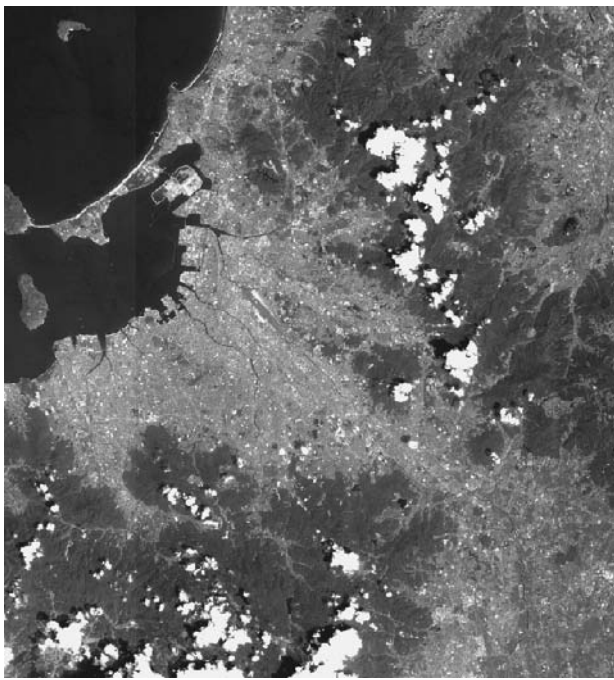


Fig. 1 Used PRISM data and its location

3.2 Data extraction from level 1B1 product

Orbit and attitude data must be extracted from the level 1B1 products to orientate PRISM images referring to the format specification (Earth Observation Research Center, JAXA, 2006).

Orbit data are recorded as positions and velocities of every 60 sec. Hermite interpolation, which is polynomial interpolation satisfying the position and velocity of sample points, was executed using 4 sample points around the scene center. Because time to the power of 7 must be calculated in the Hermite interpolation, relative time to scene center in minutes was used to reduce the calculation error.

Attitude data are recorded as quaternion in ECI (Earth Centered Inertial Coordinate System). Care is required, because the definition of quaternion in the ALOS product differs from usual. Quaternions were converted into rotation matrixes, interpolated in time space, and converted into ECR (Earth Centered Rotating Coordinate System). Information to convert from ECR to ECI is also supplied by the level 1B1 product.

3.3 Known ground points

Known ground points selected and measured by staff of the Topographic Development Office, GSI (Geographical Survey Institute) were used. They selected 49 locations within the triplet image, then selected 2 or 3 well-recognized ground points at each location. Ground coordinates of the points were measured by RTK-GPS (Fig. 2). Image coordinates of the points were measured by image interpretation on general-purpose image processing software. These 117 known ground points in total are used for control points or verification points. Figure 3 shows a sample of the record of known ground points; the location includes 3 known ground points.



Fig. 2 Observation of ground coordinates

4. Results

4.1 Before adjustment

Before the adjustment, the residuals of image observation were as listed in Table 1. The values are converted into corresponding ground length in this paper. Residuals of the verification points after the intersection, coordinates of the bundle intersection point minus measured ground coordinates, are listed in Table 2, and their residual vectors are shown in Fig. 4. All known points were used as verification points.

Residual vectors of Fig. 4 are almost the same for each radiometer, suggesting shift of the images.

4.2 Shift of the principal positions

An infinitesimal shift of the principal positions, an intersection of the optical axis and the focal plane, acts as a horizontal shift in ground space. I adjusted the principal positions of the 3 radiometers and the image observations using all known ground points as control points.

Residuals of image observation for the adjustment are listed in Table 1. Residuals of the control points after the intersection are listed in Table 2, and their residual vectors are shown in Fig. 5.

Residual vectors of Fig. 5 appear to be whirled. This suggests rotation of the radiometers on the optical axis, which cannot be derived from the shift of the principal positions.

ID:02		画像基準点の記 世界測地系(測地成果2000)			
201	緯度: 33° 27'46.30816"	座標系 X: 51565.378	標高: 448.263		
	経度: 130° 16'30.66448"	4系 Y: -67374.410	橋円体高: 481.170		
202	緯度: 33° 27'46.15451"	座標系 X: 51560.587	標高: 448.059		
	経度: 130° 16'30.98294"	4系 Y: -67366.220	橋円体高: 480.967		
203	緯度: 33° 27'45.99489"	座標系 X: 51555.610	標高: 447.852		
	経度: 130° 16'31.31423"	4系 Y: -67357.700	橋円体高: 480.759		

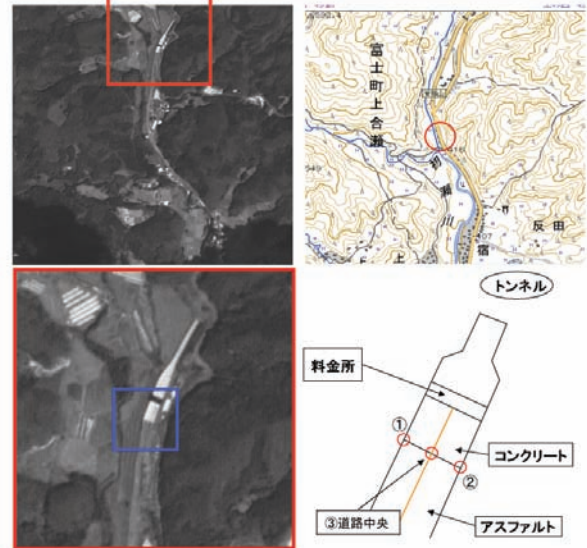


Fig. 3 Record of known ground points

Table 1 Residuals of image observation

	Before the adjustment	Adjustment of principal positions	Adjustment of rotation of the radiometers
<i>E</i> (Easting)	677.5 m	4.5 m	4.1 m
<i>N</i> (Northing)	749.5	14.6	2.6
$R = \sqrt{E^2 + N^2}$	1010.3	15.3	4.9

Note: Values are converted into corresponding ground length. The residuals are for verification points for "before the adjustment," otherwise for control points.

Table 2 Residuals of verification/control points after the intersection

	Before the adjustment	Adjustment of principal positions	Adjustment of rotation of the radiometers
<i>E</i> (Easting)	120.2 m	2.0 m	2.1 m
<i>N</i> (Northing)	713.1	8.2	2.1
<i>H</i> (Height)	258.5	16.1	3.2
$R = \sqrt{E^2 + N^2}$	723.2	8.4	2.9

Note: The residuals are for verification points for "before the adjustment," otherwise for control points.

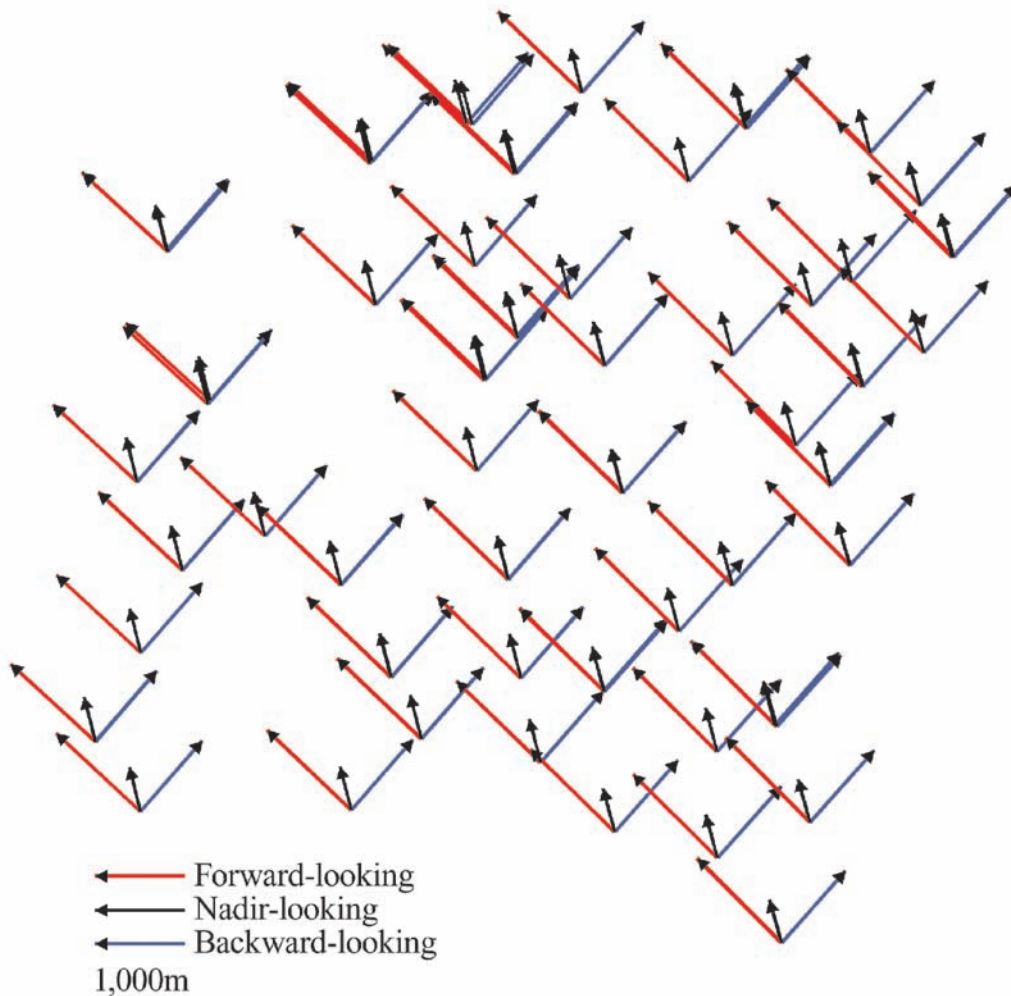


Fig. 4 Residuals of image observation (before the adjustment)

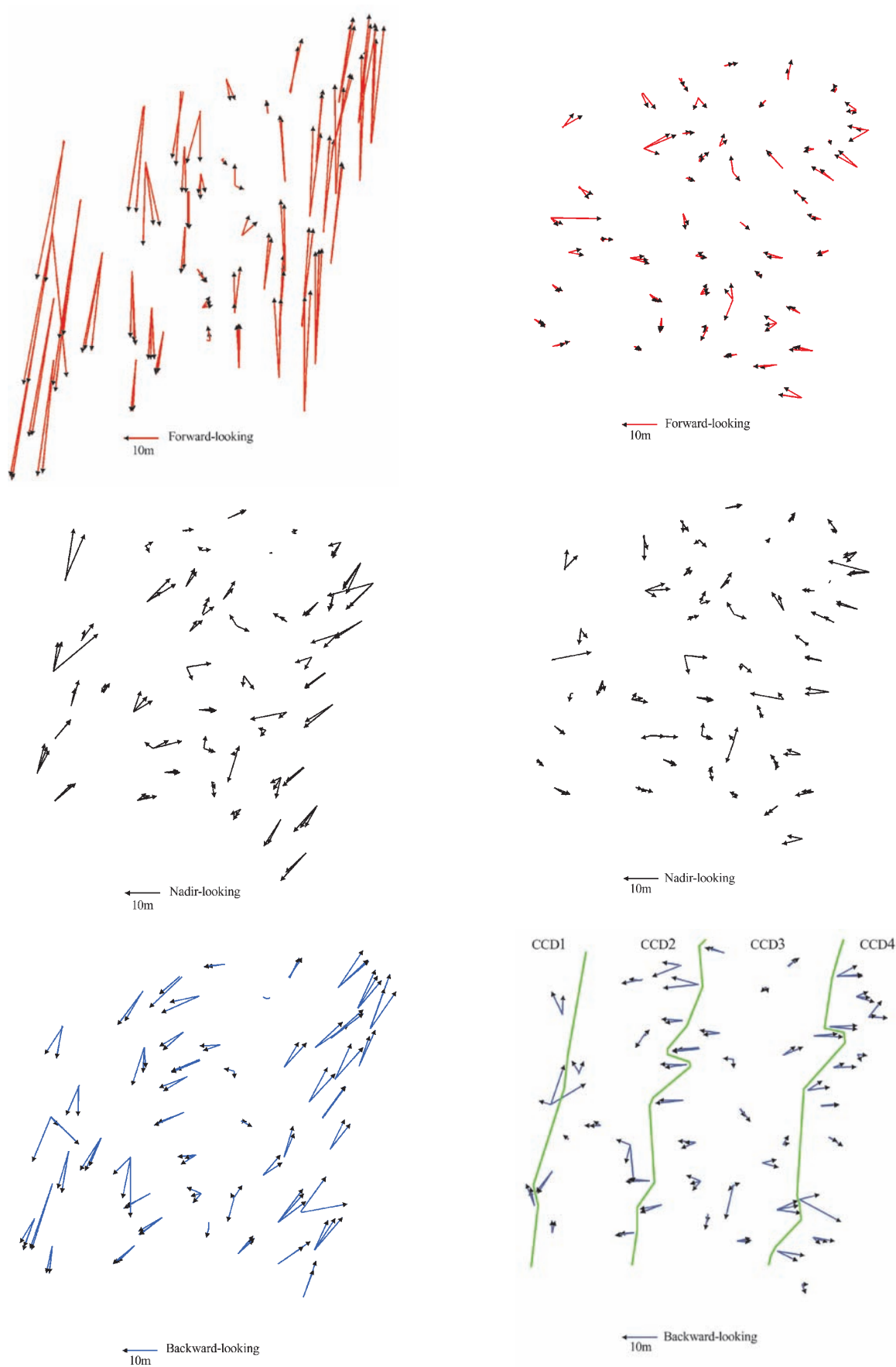


Fig. 5 Residuals of image observation (adjustment of principal positions)

Fig. 7 Residuals of image observation (adjustment of rotation of the radiometers)

4.3 Rotation of the radiometers

An infinitesimal rotation of the radiometers in satellite coordinates space acts as a horizontal shift and horizontal shear deformation in ground space (Fig. 6). Because PRISM is a push-broom sensor, yawing, which is rotation on the satellite Z axis, causes shear deformation unlike a frame sensor.

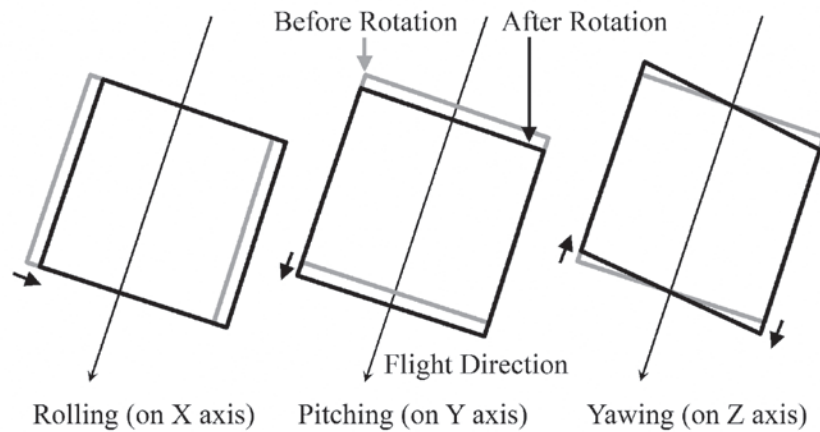


Fig. 6 Effect of radiometer rotation on ground space

5. Discussion

5.1 Residual after adjustment of radiometer rotation

Residual vectors of Fig. 7, especially backward-looking ones, seem to depend on pixel number. The boundaries between the CCDs are drawn on backward-looking of Fig. 7.

Error vectors of CCD 1 tend to be upward; those of CCD 2 tend to be neutral at left and leftward at right; those of CCD 3 tend to be leftward at left and rightward at right; and those of CCD 4 tend to be rightward.

These tendencies can be explained as shift or linear error of CCD alignment on the focal plane. The positions of 2 points near the ends of the CCDs were measured to determine CCD alignment before the launch. Both the error of the pre-launch measurement and the deformation after the measurement may cause the shift error and the linear error.

5.2 Comparison with other research

Tadono et al. (2006) reported geometric errors of PRISM images. They reported errors in the form of average and SD (standard deviation). I calculated RMSEs (Root Mean Square Errors) by square-rooting the

I adjusted the rotation of the radiometers and the image observations using all known ground points as control points.

Residuals of image observation for the adjustment are listed in Table 1. Residuals of the control points after the intersection are listed in Table 2, and their residual vectors are shown in Fig. 7.

sum of squared average and squared SD. The RMSEs are considered as absolute errors and are listed in Table 3. The SDs are considered as relative errors and are listed in Table 4.

The absolute errors correspond to residuals of image observation before the adjustment, as listed in the second column of Table 1. The relative errors correspond to residuals of image observation after adjusting the rotation of the radiometers, as listed in the last column of Table 1.

Relative errors were slightly better than those of Tadono et al. (2006), but absolute errors were much worse. The difference might have been caused by improvement of JAXA's processing system, especially geometric parameter after processing of the Fukuoka data, or by wrong implementation of my program.

The onboard clock of ALOS had a 1-second error causing 7–8 km along track error, which was repaired on September 22, after the observation of Fukuoka (Tadono et al., 2006). The clock error was corrected during the ground processing for Fukuoka's data. However, the clock error caused wrong attitude control (Tadono et al., 2006), which might affect attitude

determination and cause the difference of absolute errors.

The effect of ignoring aberration, atmospheric effect, and earth rotation is too small to explain the difference.

Tadono et al. (2006) also reported errors of CCD alignment and plotted error values of the backward radiometer against pixel number. The result is similar to Fig. 7.

Table 3 Absolute geometric error of PRISM images reported by Tadono et al. (2006)

	Forward-looking	Nadir-looking	Backward-looking
X (Along track)	10.9 m	18.7 m	28.2 m
Y (Cross track)	63.2	30.4	7.4
$R = \sqrt{E^2 + R^2}$	64.1	35.7	29.2

Table 4 Relative geometric error of PRISM images reported by Tadono et al. (2006)

	Forward-looking	Nadir-looking	Backward-looking
X (Along track)	2.3 m	1.8 m	2.2 m
Y (Cross track)	5.9	5.4	4.7
$R = \sqrt{E^2 + R^2}$	6.3	5.7	5.2

5.3 Necessary number of GCP

Many control points were used in section 4 to clarify the geometric characteristics of PRISM. However, we cannot use so many control points in actual works. The number of control points needed for geometric correction of PRISM images by rotating radiometers is considered below.

The effects of the radiometer rotation contain shear deformation as shown in Fig. 6. Control points must be distributed on both the left and right parts of the image to detect shear deformation, that is, an east–west distribution of control points is necessary.

The number of unknown parameters is 3 for each radiometer, and one control point observes 2 values, pixel number and line number, for a radiometer. Therefore, at least 2 control points are necessary to determine the parameters. There is, however, only one redundant observation for a radiometer, which is very dangerous. Consequently, it is recommended to use 2 pairs of east–west distributed control points, i.e. 4 points in total, which have 5 redundant observations for a radiometer.

6. Conclusions

The early product of ALOS PRISM had errors likely caused by rotation of radiometers and errors likely caused by mis-alignment of CCDs on the focal plane. Adjusting the rotation of the radiometers, residuals of image observation, which correspond to the accuracy of single image observation, were 4.9 meters. Residuals of control points after the intersection, which correspond to the accuracy of triplet observation, were 2.9 m in the horizontal and 3.2 m in the vertical.

East–west distributed control points are necessary to adjust the radiometer rotation. Two pairs of east–west distributed control points are recommended.

Acknowledgment

I thank the Topographic Development Office, GSI for providing the known ground points data of Fukuoka, which were essential for this study. I also thank JAXA for providing the PRISM data and related technical information under the collaboration agreement between GSI and JAXA.

References

- Eckardt, A., Braunecker, B., and Sandau, R. (2000): Performance of the imaging system in the LH systems ADS40 airborne digital sensor, *International Archives of Photogrammetry and Remote Sensing*, Vol. XXXIII, Part B1, pp. 104–109.
- Earth Observation Research Center, JAXA (2006): ALOS/PRISM Level 1 Product Format Description, Revision J, pp. 2-5-2-6, Appendix 2-7-2-19, and Appendix 3-1-3-2, http://stage.tksc.jaxa.jp/eorcalos/PRISM_L1_J_ENa.zip (accessed on December 19, 2006).
- Kamiya, I. (2005): Development of a Program for Orientation of ALOS PRISM Images and its Verification Using Simulation Data, *Journal of Applied Survey Technology*, No. 16, pp. 76–86 (in Japanese).
- Kamiya, I. (2006): Development of Orientation and DEM/Orthoimage Generation Program for ALOS PRISM, ACRS 2006 CD-ROM Proceedings.
- Tadono, T., Shimada, M., Hashimoto, T., Murakami, H., Takaku, J., and Mukaida, A. (2006): Results of Initial Calibration and Validation for ALOS Optical Sensors (PRISM and AVNIR-2), *Proceedings of the 41st Conference of the Remote Sensing Society of Japan*, pp. 129–130 (in Japanese).